

3<sup>rd</sup> CIRP Conference on Surface Integrity (CIRP CSI)

## Analysis of abrasion mechanisms in the AISI 303 stainless steel: Effect of deformed layer

V. Seriacopi<sup>a\*</sup>, N. K. Fukumasu<sup>a</sup>, R. M. Souza<sup>a</sup>, I. F. Machado<sup>a</sup>

<sup>a</sup>*Surface Phenomena Laboratory, Polytechnic School, University of Sao Paulo, Av. Prof. Mello Moraes, 2231, Sao Paulo, 05508-030, Brazil*

\*Corresponding author. Tel.: +551130919868; fax: +551130915461. E-mail address: [vanessaseriacopi@usp.br](mailto:vanessaseriacopi@usp.br)

### Abstract

Austenitic stainless steel is used in many industrial applications, especially those in which the corrosion resistance is relevant. However, this material is susceptible to surface damage, as well as the occurrence of phase transformations during manufacturing or even throughout use, since they present high work hardening. Therefore, the surface integrity cannot be neglected. This work aims studying the mechanical behavior of AISI 303 stainless steel during scratch tests. Analyses were conducted at the microstructural level, considering the presence of MnS inclusions. Scratch tests with normal loads on the order of mN were carried out using a diamond stylus to simulate the action of a single abrasive particle. The effect of surface finishing was evaluated by testing surfaces with mechanical or electrolytic polishing, which differ in terms of the presence (in the mechanical) or absence (in the electrolytic) of a deformed layer close to the specimen surface. The results allowed estimating the transition loads between abrasion mechanisms, from micro-ploughing to microcutting. These loads were determined for the different surface finishing. Preliminary numerical simulations were also included. In single abrasive operations, numerical results indicated the trend in decreasing the mass removed when the strain-hardened layer is considered.

© 2016 The Authors. Published by Elsevier B.V. This is an open access article under the CC BY-NC-ND license

(<http://creativecommons.org/licenses/by-nc-nd/4.0/>).

Peer-review under responsibility of the scientific committee of the 3rd CIRP Conference on Surface Integrity (CIRP CSI)

Keywords: Stainless Steel; Abrasion; Surface Finishing.

### 1. Introduction

The wide industrial application of austenitic stainless steels is mainly justified by their corrosion resistance [1]. The British Stainless Steel Association [2] reported their benefits in medical, pharmaceutical and food processing areas. These materials are non-magnetic and represent 65-70% of the stainless steel grades [2].

Despite the benefits regarding corrosion resistance, these materials are usually susceptible to the surface damage, as well as the occurrence of phase transformations during manufacturing or use, due to high work hardening [3]. Another unfavorable point is the mechanism of built up edge formation during cutting, which often leads to the adhesive wear of tools [4]. Thus, the surface integrity can be negatively affected depending on the tribological conditions encountered in the application. Although the stainless steel work hardening is presented as a disadvantage throughout the machining operations, many researches [5–9] have shown the high strain-hardening rate and the deformation-induced transformation as

positive aspects regarding the workpiece applications and mechanical properties.

The work conducted by Avery presented a comparison of the tribological behavior of electropolished or abraded stainless steel surfaces, considering the existence of a hardened layer in the last one [10]. Hokkirigawa, Kato and Li [11] characterized the evolution of abrasive mechanisms in austenitic stainless steels, from the mild abrasion or ploughing to the severe abrasion or cutting. In view of this background, this work aims to study the mechanical behavior of AISI 303 stainless steel during scratch tests. Analyses were conducted with loads on the order of mN, such that material behavior is affected by the presence of MnS inclusions. The effect of surface finishing was evaluated by testing surfaces with mechanical and electrolytic polishing. The results allowed estimating the transition loads between abrasion mechanisms, from micro-ploughing to microcutting [11]. These mechanisms were considered to evaluate the effect of a single abrasive on the materials microstructure. In brief, the approach in this work consists in a simplified analysis that

correlates with manufacturing operations with non-defined tool geometry, such as grinding. Moreover, preliminary numerical simulations were developed to verify possible differences concerning the experimental mass removal during the scratch tests.

## 2. Materials and Methods

**Materials.** In this work, specimens of AISI 303 and 304 were studied. The nominal chemical composition (%wt) of AISI 303 is 17.20Cr, 8.21Ni, 1.88Mn, 0.48Si, 0.05C, 0.2S and 0.04P. This composition is the result of the addition of sulfur to the composition of AISI 304 stainless steel, which contains only 0.03 %wt of sulfur, in order to obtain MnS inclusions that usually improve the material machinability [5,12]. The longitudinal sections of bars with diameter equal to 25 mm were evaluated (rolling direction). Assuming that the austenitic matrix of both materials is similar, Vickers microhardness tests were conducted only on AISI 304, to get information from the steel matrix, avoiding the effect of the higher volume fractions of MnS. This procedure allows comparison with literature results [10,11]. Furthermore, scratch tests were conducted only on AISI 303 specimens.

**Surface finishing preparation.** The microstructure of AISI 303 steel was observed by scanning electron microscopy (SEM - Jeol JSM 6010-LA) with energy dispersive X-ray spectroscopy (EDS). Specimen preparation consisted of mechanical or electrolytic polishing. Mechanical polishing causes a strain-hardened layer that can be removed by electrolytic polishing. Therefore, two different conditions at the surface and subsurface were obtained.

The mechanical polishing consisted of grinding and polishing down to 0.04  $\mu\text{m}$  colloidal silica suspension. Further electrolytic polishing was carried out in one sample. The electrolyte composition was: 800 mL of ethyl alcohol, 140 mL of distilled water and 60 mL of perchloric acid. The electrolyte was kept below 10  $^{\circ}\text{C}$  and samples were polished at 40 V for 20 s. The area exposed was 1  $\text{cm}^2$ , following the literature recommendations [13].

**Mechanical properties evaluation.** Vickers microhardness tests were conducted on the AISI 304 steel specimen, selecting loads of 50, 100, 500 and 2,000 gf. One-Way analysis of variance was performed to calculate the pre-hardened layer thickness in view of the different depths of penetration [14,15].

**Scratch tests.** Scratch tests were conducted on AISI 303 samples in order to study the action of a single abrasive at the microscale. TI-950 Hysitron triboindenter was applied for these tests. The High Load module was selected and tests were conducted with constant normal forces. The scratch test stylus was a diamond conical indenter with 5  $\mu\text{m}$  tip radius and internal angle of  $\sim 60^{\circ}$ . The scratch procedure consisted of the following steps: (i-) surface profilometry; (ii-) indentation or loading; (iii-) scratching; and (iv-) unloading. The scratch length was 400  $\mu\text{m}$ , with 10  $\mu\text{m}\cdot\text{s}^{-1}$  linear velocity. Two repetitions were performed for each normal load.

The range of normal forces applied during the scratches was selected based on the abrasion mechanisms map reported by Hokkirigawa, Kato and Li [11]. Therefore, the range from 5 to 50 mN was estimated to cover all the abrasive mechanisms (see Figure 1). The degree of penetration ( $D_p$ ) in Figure 1 is a parameter that indicates the severity of mass removal and can be determined using Eq. (1) [11], where: R is the tip radius of the abrasive (5  $\mu\text{m}$ ); H is the slab hardness (200 HV); and W is the normal force (from 5 to 100 mN).

$$D_p = R \left( \frac{\pi H}{2W} \right)^{1/2} - \left( \frac{\pi R^2 H}{2W} - 1 \right)^{1/2} \quad (1)$$

After the scratch tests, AISI 303 steel specimens were characterized by SEM, and by Coherence Correlation Interferometry (CCI-MP Taylor Hobson), which allowed evaluating the 3D topography.

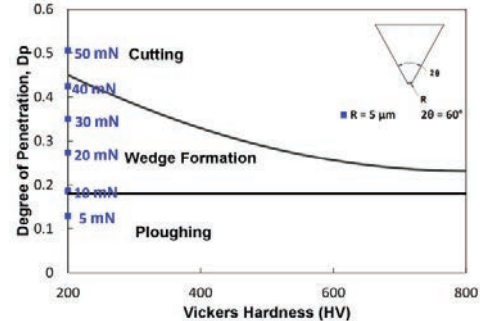


Fig. 1. Abrasion mechanisms estimated for the homogeneous austenitic stainless steel (AISI 304) in view of Hokkirigawa, Kato and Li's work [11].

**Computational Simulation.** A two-dimensional (2D) numerical model of the scratch tests was developed using the Finite Element Method (FEM), in Abaqus/Explicit 6.13<sup>®</sup> software. Plane stress and constant normal force were considered throughout the scratches. The abrasive particle was modeled with a 5  $\mu\text{m}$  tip radius and with a rigid-analytical surface. Four materials were tested as the slab: the homogeneous case (304 steel - austenitic matrix), with and without the presence of the strain-hardened layer; and the heterogeneous material (303 steel - austenitic matrix with MnS), with and without the effect of that previously calculated strain-hardened layer. It was assumed that the slab phases (matrix and sulfides) were elastic-plastic, with mechanical properties (modulus of elasticity, yield stress and strain-hardening coefficient) obtained by experimental instrumented indentation, using 10 mN load. The densities and Poisson ratio were obtained in the literature [16,17]. The damage parameters for nucleation and propagation were specified according to the literature [18]. In each simulation, the slab was discretized with quadrilateral elements (CPE4R type). The smallest element of the mesh had an edge of 0.5  $\mu\text{m}$ .

## 3. Results

### 3.1. Surface Finishing Characterization

Figure 2 displays the structure of the longitudinal section of the AISI 303 steel bar, characterized by SEM and EDS. The figure indicates an austenitic matrix and MnS inclusions. In addition, composition maps from EDS analysis show higher levels of Mn and S in the inclusions, denoted by the color scales. Five measurements of the 3D topography were carried out in different areas of the surfaces of each sample. The calculated topography parameters are displayed in Table 1. Values indicate that the electropolished surface is rougher, has a higher density of peaks, and sharper asperities. Bhuyan et al. [19] reported that a more efficient control of the electrolytic polishing parameters, such as electrolyte temperature, current density, polishing time and pulsed current application, is necessary to adjust the flatness and to avoid the majority of pitting formation on these surfaces.

Download English Version:

<https://daneshyari.com/en/article/1698507>

Download Persian Version:

<https://daneshyari.com/article/1698507>

[Daneshyari.com](https://daneshyari.com)